Available online at www.sciencedirect.com
SCIENCE DIRECT®
ELSEVIER
Agricultural and Forest Meteorology 118 (2003) 207–220
AGRICULTURAL AND FOREST METEOROLOGY
www.elsevier.com/locate/agrformet

Assessing soil CO_2 efflux using continuous measurements of CO_2 profiles in soils with small solid-state sensors

Jianwu Tang*, Dennis D. Baldocchi, Ye Qi, Liukang Xu

Department of Environmental Science, Policy, and Management, 145 Mulford Hall, University of California at Berkeley, Berkeley, CA 94720, USA

Received 2 December 2002; received in revised form 1 April 2003; accepted 7 April 2003

Abstract

This paper describes a new method to monitor continuously soil CO_2 profiles using small solid-state CO_2 sensors buried at different depths of the soil. Based on the measurement of soil CO_2 profile and a gaseous diffusivity model, we estimated soil CO_2 efflux, which was mainly from heterotrophic respiration, and its temporal variation in a dry season in a Mediterranean savanna ecosystem in California. The daily mean values of CO_2 concentrations in soils had small variation, but the diurnal variation was significant and correlated well with soil temperature. The daily mean CO_2 concentration remained steady at 396 μmol mol^{-1} at 2 cm depth during the dry summer from days 200 to 235 in 2002. Over the same period, CO_2 concentration decreased from 721 to 611 μmol mol^{-1} at 8 cm depth, and from 1044 to 871 μmol mol^{-1} at 16 cm. The vertical soil CO_2 concentrations changed almost linearly with depth up to 16 cm, but the gradient varied over time. Based on the soil CO_2 gradient and the diffusion coefficient estimated from the Millington–Quirk model, continuous soil CO_2 efflux was calculated. The daily mean values of CO_2 efflux slightly decreased from 0.43 to 0.33 μmol m^{-2} s^{-1} with a mean of 0.37 μmol m^{-2} s^{-1}. The mean diurnal range of CO_2 efflux was greater than the range of daily mean CO_2 efflux within the study period. The diurnal variation of soil CO_2 efflux ranged from 0.32 to 0.45 μmol m^{-2} s^{-1} with the peak value reached between 14:30 and 16:30 h. This pattern corresponded well with the increase in soil temperatures during this time. By plotting CO_2 efflux vs. soil temperature, we found that CO_2 efflux correlated exponentially with soil temperature at the depth of 8 cm, with R^2 of 0.86 and Q_{10} of 1.27 in the summer dry season. The Q_{10} value increased with the depth of soil temperature measurements. The high correlation between CO_2 efflux and temperature explains the diurnal pattern of CO_2 efflux, but moisture may become another factor driving the seasonal pattern when moisture changes over seasons. The estimated CO_2 efflux using this method was very close to chamber measurements, suggesting that this method can be used for long-term continuous measurements of soil CO_2 efflux.

Keywords: CO_2 profile; CO_2 efflux; Soil respiration; Diffusion; CO_2 sensor; Soil CO_2 concentration

1. Introduction

Soil surface CO_2 efflux, or soil respiration, is a major component of the biosphere's carbon cycle because it may constitute about three-quarters of total ecosystem respiration (Law et al., 2001). In recent years, soil CO_2 efflux has been the subject of intense studies because of its potential and controversial role in amplifying global warming (e.g. Trumbore et al., 1996; Liski et al., 1999; Cox et al., 2000; Giardina and Ryan, 2000; Kirschbaum, 2000; Luo et al., 2001). Soil carbon modelers generally view soil CO_2 efflux as a

* Corresponding author. Tel.: +1-510-643-3263; fax: +1-510-643-5438.
E-mail address: jtang@nature.berkeley.edu (J. Tang).

0168-1923/$ – see front matter © 2003 Elsevier Science B.V. All rights reserved.
doi:10.1016/S0168-1923(03)00112-6

function of soil temperature or a combination of soil temperature and moisture (e.g. Raich and Schlesinger, 1992; Davidson et al., 1998; Epron et al., 1999; Treonis et al., 2002). However, there is no consensus in functional forms and parameterization in these models. The uncertainty is partly due to the instrumentation and methods used to measure soil CO_2 production and efflux (Livingston and Hutchinson, 1995; Davidson et al., 2002).

Information on soil respiration is also needed to interpret eddy covariance measurements, which are now being acquired on a quasi-continuous basis across the global FLUXNET network (Baldocchi et al., 2001). The eddy covariance method measures ecosystem productivity (NEP), a net result of photosynthesis and respiration, but it does not provide individual information such as photosynthesis, autotrophic respiration, and heterotrophic respiration (though nighttime eddy covariance data provide information on ecosystem respiration in the dark). Since these processes have different mechanisms and environmental drivers, partitioning of eddy covariance data has received much attention (Piovesan and Adams, 2000). Continuous eddy covariance measurements of CO_2 fluxes need continuous soil CO_2 measurements at a similar frequency (per half-hour) in order to decompose NEP, understand temporal variation, and explain some unusual episodic events that are observed.

Methods of soil CO_2 efflux measurement are still in development. An early method periodically extracts soil gas samples from different depths to study CO_2 profile and diffusion (De Jong and Schapper, 1972; Wagner and Buyanovsky, 1983; Burton and Beauchamp, 1994; Davidson and Trumbore, 1995). The gas extraction method can provide information on soil CO_2 production at several depths, but it cannot provide in situ, continuous and convenient data on CO_2 efflux. Furthermore, this method will disturb the soil environment. An unavoidable bias may occur during the processes of gas extraction, storage, transport, and measurement.

Chamber-based measurements allow us to directly measure CO_2 efflux from soils on a small scale (e.g. Meyer et al., 1987; Norman et al., 1992). Fixed chambers and portable chambers have evolved into automated systems for continuous and semi-continuous measurements (Goulden and Crill, 1997; Russell et al., 1998; Scott et al., 1999; Drewitt et al., 2002; King and Harrison, 2002). Shortcomings with closed-chamber methods, however, still exist. Efflux readings may be biased by disturbing air pressure and altering CO_2 concentration in the soil (Livingston and Hutchinson, 1995; Healy et al., 1996; Davidson et al., 2002). By measuring accumulation of soil CO_2 productivity released from the soil surface, chambers are unable to provide information about soil profiles and individual contributions at certain soil depths, which is important for understanding soil carbon mechanisms. Currently, no reliable and robust automated chambers for field measurements are commercially available.

Understory eddy covariance towers provide an alternative to continuously measure soil CO_2 efflux without disturbing the soil (Baldocchi and Meyers, 1991; Law et al., 1999). As with overstory eddy covariance techniques, understory eddy covariance measurement may face difficulty in measuring respiration at night when turbulence is weak and intermittent and drainage flows dominate the transfer of CO_2 (Goulden et al., 1996; Moncrieff et al., 1997). Compared with overstory eddy covariance, the low height of understory towers corresponds with small areas of footprint, which may induce errors when large areas of ecosystems are represented. Furthermore, understory eddy covariance data cannot separate soil CO_2 efflux, bole respiration below sensors, and overlying herbaceous vegetation, when it is present.

Partitioning NEP into GPP (gross primary productivity) and NPP (net primary productivity), and partitioning soil respiration into autotrophic and heterotrophic respiration are of critical importance for building process-based models since these components respond differently to abiotic and biotic drivers. Despite the development of methods such as trenching and isotopic approaches for partitioning the source of soil CO_2 (Hanson et al., 2000), few studies have directly measured and modeled heterotrophic respiration in situ without any disturbance. As a result, studies on temperature sensitivity (Q_{10}) of soil CO_2 efflux often combine heterotrophic respiration with autotrophic respiration (e.g. Raich and Schlesinger, 1992; Lloyd and Taylor, 1994; Xu and Qi, 2001), which may vary with plant physiological and phenological factors other than temperature. Thus, correlation coefficients between soil CO_2 efflux and temperature often have low values. Savanna ecosystems with dead grasses and live but sparse trees in the summer provide a unique opportunity to measure and model heterotrophic respiration. However, publications on heterotrophic respiration in savannas are limited.

Due to the limitation of instrumentation, particularly due to the large size of commonly used infrared gas analyzers, there are very few publications on continuous measurements of CO_2 profile in the soil. Recently, an innovative CO_2 sensor was developed for air quality monitoring and control. This instrument has the potential to be buried in the soil and measure CO_2 in the soil atmosphere. Hirano et al. (2000) first used a type of these small CO_2 sensors (GMD20, Vaisala Inc., Finland) buried in the soil under a deciduous broad-leaved forest in Japan to deduce soil respiration, and therefore have demonstrated the feasibility of the instrument.

In order to develop more measurement methods in soil CO_2 efflux, this paper describes in detail the use of the new small solid-state CO_2 sensors (GMT222, Vaisala Inc., Finland) to continuously monitor soil CO_2 profiles and soil CO_2 efflux by burying these CO_2 sensors at different soil depths. Based on the measurement of the CO_2 profile and a diffusivity model, we estimated rates of soil CO_2 efflux in a dry season in a Mediterranean savanna ecosystem in California. The relationship between CO_2 efflux and soil temperature was explored. Soil CO_2 efflux measurements by chambers were used to validate this method.

2. Materials and methods

2.1. Site description

The field study was conducted at an oak-grass savanna (38.4311°N, 120.9660°W and 177 m), one of the Ameriflux sites, located at the lower foothills of the Sierra Nevada Mountains near Ione, California. The climate is Mediterranean, hot and dry with almost no rain in the summer and relatively cold and wet in the winter. Mean annual temperature and precipitation over the recent 30 years at a nearby weather station with similar altitude and vegetation are 16.3 °C and 558.7 mm, respectively.

The overstory of the oak savanna consists of scattered blue oak trees (*Quercus douglasii*), with occasional gray pine trees (*Pinus sabiniana*) ($3\,ha^{-1}$). The understory landscape has been managed, as the local rancher has removed brush and the cattle graze the herbs. The main grass and herb species include *Brachypodium distachyon*, *Hypochaeris glabra*, *Bromus madritensis*, and *Cynosurus echinatus*.

A demographic survey on stand structure was conducted on a 100 m × 100 m plot of the savanna and along a 200 m transect in 2000 (Kiang, 2002). The mean height of the forest stand was 7.1 m, its mode was 8.6 m, and the maximum height was 13.0 m. The landscape supported 194 stems per hectare, whose mean diameter at breast height (DBH) was 0.199 m and basal area was $18\,m^2\,ha^{-1}$. The oak tree leaves out normally at the end of March. In about 2 weeks, its leaf area index (LAI) reaches its maximum value at about 0.6 in 2001. The growing of the understory grass is confined in the wet season, usually from the end of October to the middle of May in the next year. The maximum LAI of the grass is around 1.0. The grass was dead while this study was conducted.

2.2. Soils

The soil of the oak-grass savanna is an Auburn very rocky silt loam (Lithic haploxerepts). The soil profile is about 0.75 m deep, and overlays fractured rock. In the open area the soil is composed of 48% of sand, 42% of silt, and 10% of clay with a bulk density of $1.64\,g\,cm^{-3}$, and 0.92% of C and 0.10% of N, while under canopy the soil is composed 37.5% of sand, 45% of silt, and 17.5% of clay with a bulk density of $1.58\,g\,cm^{-3}$, and 1.09% of C and 0.11% of N. Soil texture and chemical composition were analyzed at DANR Analytical Laboratory, University of California, Davis.

2.3. Environmental measurements

Air temperature and relative humidity were measured with a platinum resistance thermometer and solid-state humicap, respectively (model HMP-45A, Vaisala, Helsinki, Finland). Static pressure was measured with a capacitance analog barometer (model PTB101B, Vaisala, Helsinki, Finland). Volumetric soil moisture content was measured continuously in the field at several depths in the soil with frequency domain reflectometry sensors (Theta Probe model ML2-X, Delta-T Devices, Cambridge, UK). Sensors were placed at various depths in the soil (5, 10, 20 and 50 cm) and were calibrated using the gravimetric method. Profiles of soil moisture (0–15, 15–30, 30–45 and 45–60 cm) were made periodically and manually using an enhanced time domain reflectometer (Moisture Point, model 917, E.S.I. Environmental Sensors Inc., Victoria, Canada). Ancillary meteorological and soil physics data were acquired and logged on CR-23x and CR-10x dataloggers (Campbell Scientific Inc., Utah, USA). The sensors were sampled every second, and half-hour averages were computed and stored on a computer to coincide with the flux measurements.

2.4. Soil CO_2 profile measurements

We built a 42.5 m transect between two oak trees in the savanna, and installed CO_2 sensors in the soil at an open area near the midpoint of the transect. Since the nearest oak trees were more than 20 m away from the sensors, the impact of oak root respiration on soil CO_2 measurements was minimal. Because the annual grasses were dead during the study period, it was safe to assume that all of CO_2 emanating from the soil is due to heterotrophic respiration.

We used solid-state CO_2 sensors (GMT222, Vaisala, Finland) to measure CO_2 profiles in the soil. The CO_2 sensor consists of three parts, a remote probe, a transmitter body, and a cable. The probe is a new silicon-based, non-dispersive infra-red (NDIR) sensor for the measurement of CO_2 based on the patented CARBOCAP® technique. Using the same working principle as other high performance large NDIR analyzers, it assesses CO_2 concentration by detecting the attenuate of single-beam dual-wavelength infra-red light across a fixed distance. The sensor is small because the CARBOCAP® sensor possesses a tiny electrically controlled Fabry–Perot interferometer (FPI) made of silicon, replacing the traditional rotating filter wheel in larger scale NDIRs. Therefore, a true dual-wavelength measurement can be made by a simple and small sensor (http://www.vaisala.com).

The feature of the probe provides us with a new and novel means of measuring soil CO_2 concentration profiles and deducing estimation of CO_2 efflux by burying the probe (sensor) in the soil. The probe is a cylinder with 15.5 cm in length and 1.85 cm in diameter. Tiny holes on the surface of the probe allow CO_2 to diffuse three-dimensionally through membranes into the sensor. In order to measure CO_2 concentration at some specific depth of soil, we encased the probe with an aluminum pipe with the same length but 5 mm larger in diameter. The casing was sealed with the probe on the upper end using a rubber gasket. The opening on the lower end allowed CO_2 molecule to diffuse to the sensor at the buried depth for CO_2 concentration measurement. The encased probe could respond to the change of CO_2 concentration in soils less than 5 min. We buried three sensors at depths of 2 cm (with a range of 0–5000 μmol mol^{-1}), 8 cm (0–10 000 μmol mol^{-1}), and 16 cm (0–10 000 μmol mol^{-1}), respectively; they were separated horizontally by about 2 cm. A schematic of the system is shown in Fig. 1.

The cable connected the probe in the soil with the transmitter body placed on the ground. After receiving the signal from the probe, the transmitter sends the output signal both to a datalogger (CR-23x, Campbell Scientific Inc., Utah, USA) and to an optional LCD display on the transmitter for the CO_2 concentration reading. We used custom-built thermocouple sensors to monitor soil temperature at the same depth where the CO_2 sensors were buried. Outputs from the probe and thermocouples were scanned every 30 s, and 5 min means were stored in the datalogger.

The system was powered by 24 V dc provided by two 12 V batteries connected in series, which were continuously charged by a 24 V photovoltaic system. Each CO_2 sensor consumes less than 4 W. The system was installed and tested in March 2002 and started to collect data on June 20, 2002. To avoid the potential impact from soil disturbance on the soil CO_2 measurements, only data collected after July 19, 2002 were included in the analysis of this study.

The GMT222 CO_2 sensor is a kind of GMT220 series sensors that have measurement range options from 0–2000 μmol mol^{-1} to 0–20%. The technical specifications indicate an operating temperature ranging from -20 to 60 °C, and the accuracy of GMT222 is $\pm$20 μmol mol^{-1} plus 2% of reading. We calibrated the sensors using lab standards that are traceable to the NOAA/CMDL standards, and found that the shift of spans were in the specification range.

2.5. Data analysis

In order to decrease the systematic error, the concentration readings from the CO_2 sensor need to be

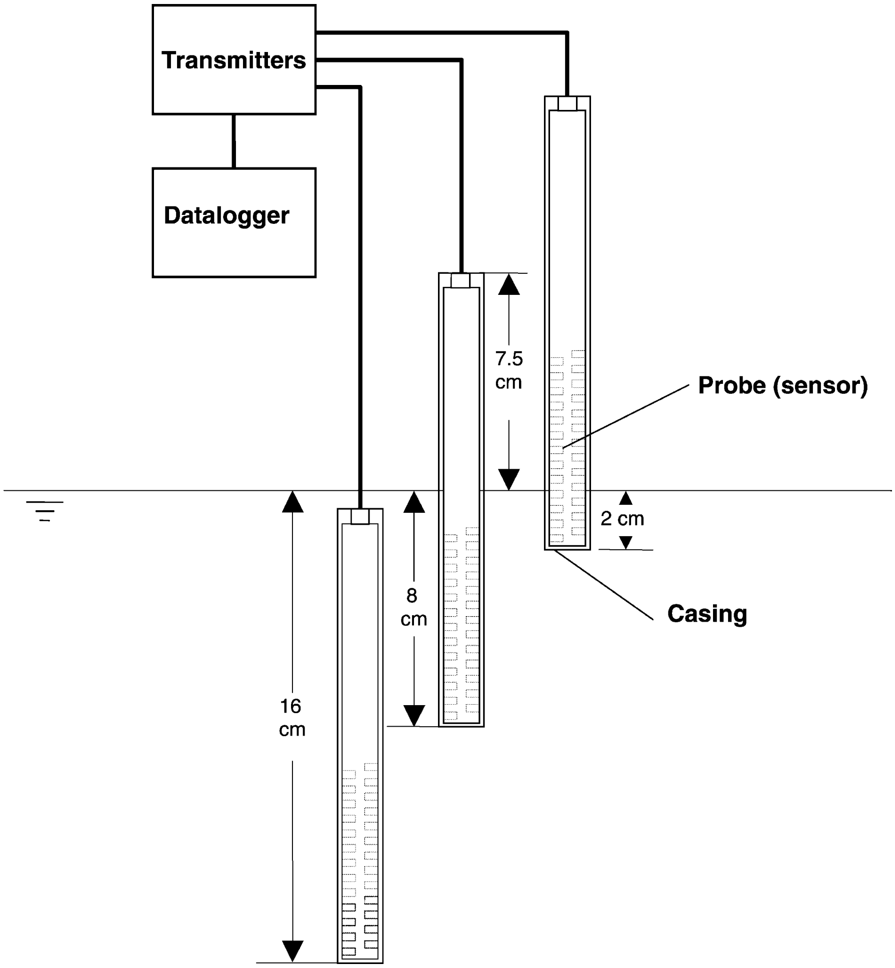

Fig. 1. A schematic of the system for measuring soil CO_2 profile using solid-state CO_2 sensors. The encased probes are buried in the soil at three depths. The transmitters are placed on the ground receiving signals from the probes and sending to the datalogger.

corrected for variations in temperature and pressure. The reference temperature and pressure for the sensor are 25 °C and 101.3 kPa, respectively. Based on the ideal gas law and instrument specifications, the manufacturer of the sensor (personal communication with Dick Gronholm, Vaisala Inc. in California) provided the following empirical formulas for correcting for temperature and pressure applicable to GMT222 sensors:

$$C_c = C_m - C_T - C_P, \quad (1)$$

where C is the CO_2 concentration in μmol mol^{-1}, and the subscripts c, m, T, and P stand for corrected, measured, temperature correction, and pressure correction.

The temperature correction was computed by

$$C_T = 14\,000(K_T - K_T^2)\left[\frac{25 - T_c}{25}\right], \quad (2)$$

where T_c is the temperature (°C), and $K_T = A_0 + A_1 \times C_m + A_2 \times C_m^2 + A_3 \times C_m^3$, $A_0 = 3 \times 10^{-3}$, $A_1 = 1.2 \times 10^{-5}$, $A_2 = -1.25 \times 10^{-9}$, $A_3 = 6 \times 10^{-14}$.

The pressure correction was computed by

$$C_P = K_P\left[\frac{P - 101.3}{101.3}\right], \quad (3)$$

where P is the pressure (kPa), and $K_P = A \times C_m$, $A = 1.38$.

The data collected from CO_2 sensors are in volume fraction (μmol mol^{-1}), which can be changed to mole concentration (μmol m^{-3}). The flux of CO_2 diffused from the soil can be calculated by Fick's first law of diffusion:

$$F = -D_s \frac{dC}{dz}, \tag{4}$$

where F is the CO_2 efflux (μmol m^{-2} s^{-1}), D_s the CO_2 diffusion coefficient in the soil (m^2 s^{-1}), C the CO_2 concentration (μmol m^{-3}), and dC/dz the vertical soil CO_2 gradient.

D_s can be estimated as

$$D_s = \xi D_a, \tag{5}$$

where ξ is the gas tortuosity factor, and D_a the CO_2 diffusion coefficient in the free air.

The effect of temperature and pressure on D_a is given by

$$D_a = D_{a0}\left(\frac{T}{293.15}\right)^{1.75}\left(\frac{P}{101.3}\right), \tag{6}$$

where T is the temperature (K), P the air pressure (kPa), D_{a0} a reference value of D_a at 20 °C (293.15 K) and 101.3 kPa, and is given as 14.7 mm^2 s^{-1} (Jones, 1992).

There are several empirical models in the literature for computing ξ (Sallam et al., 1984). We used the Millington–Quirk model (Millington and Quirk, 1961):

$$\xi = \frac{\alpha^{10/3}}{\phi^2}, \tag{7}$$

where α is the volumetric air content (air-filled porosity), ϕ the porosity, sum of α and the volumetric water content (θ). Note,

$$\phi = \alpha + \theta = 1 - \frac{\rho_b}{\rho_m}, \tag{8}$$

where ρ_b is the bulk density, and ρ_m the particle density for the mineral soil.

Eqs. (5)–(8) are used to compute the soil CO_2 diffusion coefficient D_s. ρ_b at the site was measured as 1.64 g cm^{-3}, and typical ρ_m of 2.65 g cm^{-3} was used. Thus $\phi = 1-1.64/2.65 = 0.38$. A continuous θ measured at the 5 cm depth was used to represent the average between 0 and 16 cm to compute α and thus ξ by applying the Millington–Quirk model. Free air D_a is adjusted by soil temperature at 8 cm depth and air pressure.

2.6. Soil CO_2 efflux measurements by closed chambers

To validate the above method, CO_2 efflux from the soil surface was also manually and periodically measured by chambers across the transect. Eleven soil collars, each with a height of 4.4 cm and a diameter of 11 cm, were inserted into the soil along the transect and used to measure CO_2 efflux. Soil CO_2 efflux was measured using a soil chamber (LI-6400-09, LI-COR Inc., Nebraska, USA) connected to a portable photosynthesis system (LI-6400, LI-COR Inc., Nebraska, USA) for data collection and storage. Soil CO_2 efflux was measured 1 day for every 2 weeks. The averaged CO_2 efflux measurements of two locations closest to the solid-state CO_2 sensors on days 200, 214, and 235 were used to validate estimated CO_2 efflux from these CO_2 sensors.

3. Results and discussion

3.1. CO_2 profile in measurements

Fig. 2 shows seasonal patterns with daily mean values between days 200 and 235 in 2002 of (a) CO_2 concentrations at three depth, (b) soil CO_2 efflux, (c) soil temperature, (d) soil volumetric water content, and (e) diffusion coefficient. In Fig. 2a we plotted half-hour average of CO_2 concentration at depths of 2, 8 and 16 cm and their daily mean values. During the study period, the daily mean values of CO_2 did not vary significantly at the depth of 2 cm, but decreased slightly at the depth of 8 and 16 cm. At the depth of 2 cm, the daily mean CO_2 concentration varied between 386 and 403 μmol mol^{-1} with an average over 36 days of 396 μmol mol^{-1}. The daily mean CO_2 concentration decreased from 721 to 611 μmol mol^{-1} at the depth of 8 cm; it decreased from 1044 to 871 μmol mol^{-1} at the depth of 16 cm. Daily mean soil temperature measured at the depth of 8 cm varied from 32.6 to 38.3 °C during these days (Fig. 2c), but the variation of the temperature curve did not indicate the synchronous pattern with the daily mean concentration curves. Soil volumetric moisture at the depth of 5 cm had no significant

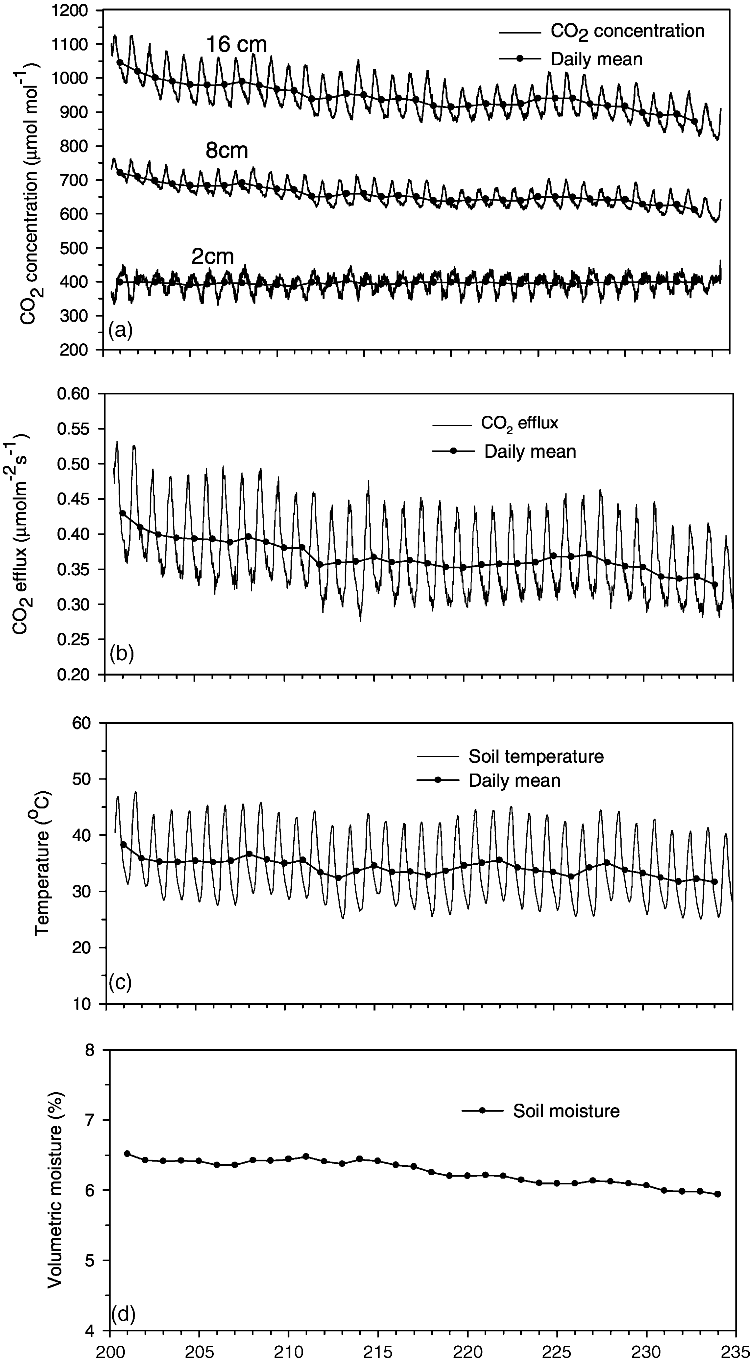

Fig. 2. Seasonal patterns with daily mean values between days 200 and 235 in 2002. (a) CO_2 concentrations in the soil at depths of 2, 8, and 16 cm; (b) soil CO_2 efflux; (c) soil temperature at the depth of 8 cm; (d) soil volumetric moisture at the depth of 5 cm; (e) diffusion coefficient.

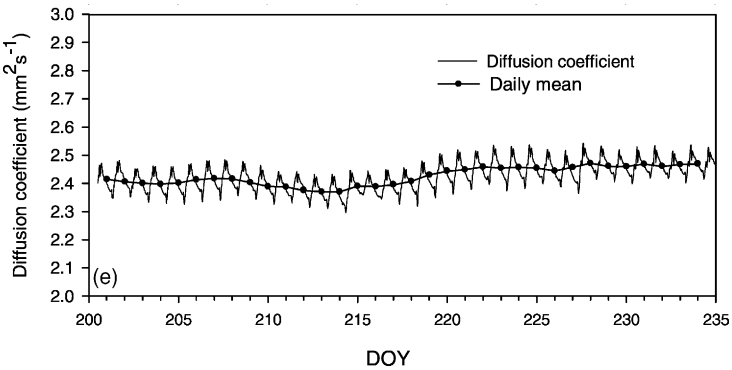

Fig. 2. (*Continued*).

diurnal variation (Fig. 2d), and it decreased slightly from 6.5 to 5.9% with an average of 6.3% over the 36-day drying period.

The decrease in soil CO_2 concentration at the depth of 8 and 16 cm probably attributed to the continuous decrease in soil moisture and carbon content at these two levels. At the depth of 2 cm, soil moisture did not change since moisture was already at a threshold value of about 5%. Thus the daily mean CO_2 concentration indicated no decrease at the depth of 2 cm.

Unlike the seasonal patterns of the soil CO_2 profile, the diurnal variation of the soil CO_2 profile was significant and correlated well with soil temperature. We computed mean diurnal patterns of soil CO_2 concentration and temperature at three depths, and their standard deviations over 34 days between days 201 and 234 (Fig. 3a and c). The 8 and 16 cm CO_2 concentration curves indicated a similar temporal pattern while the 2 cm curve showed differently. During the time 14:30–16:30 h when soil temperature was the highest within a day, the 8 cm curve and 16 cm curve reached the peak values, while the 2 cm CO_2 curve had a minimum value during this time. Temperature curves at the various depths did not peak at the same time. The temperature at 2 cm peaked early while the temperature at 16 cm peaked late. Correspondingly, the CO_2 concentration curve at 8 cm peaked earlier than that at 16 cm. The amplitudes of three temperature waves are also different with the greatest at 2 cm and the least at 16 cm.

The value of CO_2 concentration is mainly determined by the rate of CO_2 production in a certain layer of the soil and by vertical diffusion of CO_2 in and out of the layer if we neglect the horizontal transport. The 8 and 16 cm curves correlated positively with soil temperature but not the 2 cm curve. This may be explained by the CO_2 production rate and diffusivity at 2 cm. CO_2 production rates are sensitive to soil temperature, but temperature sensitivity and CO_2 production rates may decrease with the further increase in temperature (Singh and Gupta, 1977; Lloyd and Taylor, 1994; Kirschbaum, 1995; Xu and Qi, 2001). At the top soil layer, the soil temperature can be as high as 50 °C in the early afternoon. Thus the 2 cm CO_2 concentration curve did not peak in the early afternoon probably due to the extremely high temperature. Another reason for the decreased CO_2 concentration under high temperature is the transport of CO_2. The high transport rate of CO_2 may prevent the CO_2 from building-up at the top layer during early afternoon because CO_2 diffusivity increases with temperature. In addition to soil biological and physical factors, the low ambient CO_2 concentration in the afternoon (data not shown) due to tree's photosynthesis and well mixing in the atmospheric boundary layer may reduce soil CO_2 concentration at the top layer. The pressure fluctuation caused by the surface wind may also affect CO_2 concentration and CO_2 efflux through the pressure pumping effect (Massman et al., 1997).

3.2. Soil CO_2 gradients

The vertical CO_2 gradient (dC/dz) was approximately a constant at different depths of soil in our site for the field conditions experienced during this study. By plotting CO_2 concentrations vs. depth, we

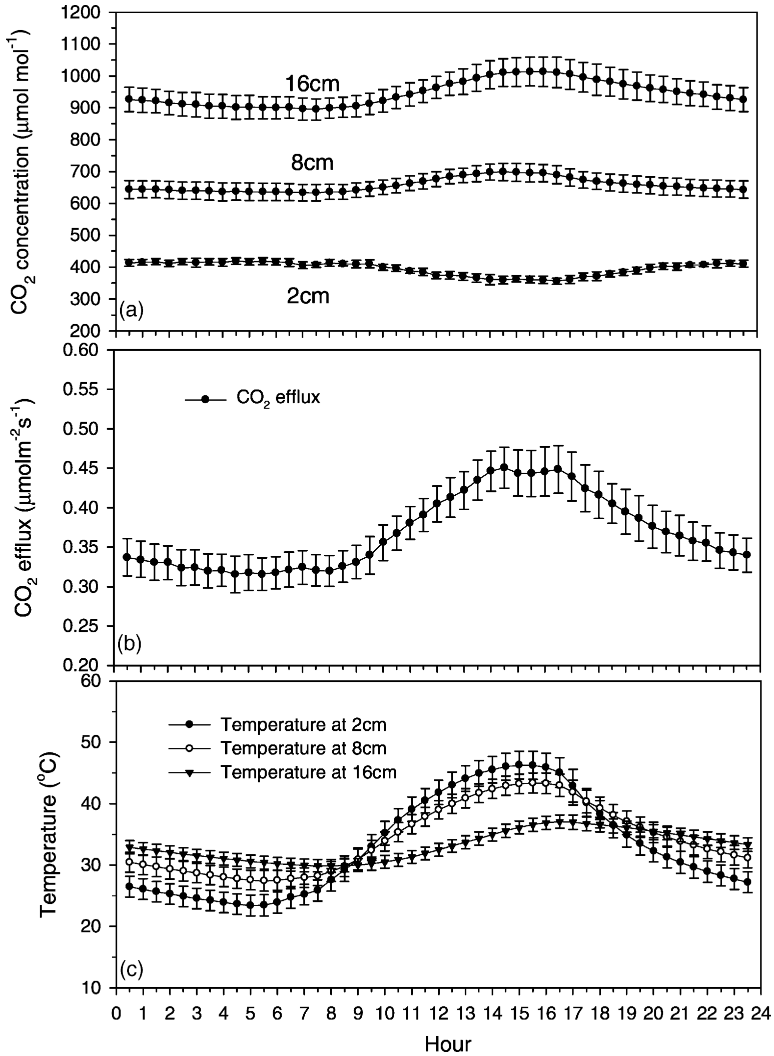

Fig. 3. Mean diurnal patterns and their standard deviations ($n = 34$) between days 201 and 234 in 2002. (a) CO_2 concentrations in the soil at depths of 2, 8, and 16 cm; (b) soil CO_2 efflux; (c) soil temperature at depths of 2, 8, and 16 cm.

found the CO_2 concentration linearly increased with depth up to 16 cm. Thus, through linear regression for CO_2 concentration over depth we computed the slope, which was used to represent CO_2 concentration gradient. The gradient changed over time. We conducted linear regressions for computing the gradient and R^2 for each 5 min period. The averaged R^2 over 10 090 regressions between days 200 and 235 was 0.997.

The linearity of CO_2 gradient makes its calculation simple, with a finite difference ($\mathrm{d}C/\mathrm{d}z = \Delta C/\Delta z$); this approximation may not be valid at deeper soil depths and during other seasons. Soil CO_2 concentration will increase with depth until reaching a certain level where CO_2 concentration may either keep a constant if a barrier is present, or decrease if there is no barrier (Jury et al., 1991). The gradient will vary with soil temperature, moisture and carbon content.

3.3. Estimation of soil CO_2 diffusivity

The average of the soil CO_2 diffusion coefficient over the depth of 0–16 cm was computed by the

Millington–Quirk model (Eq. (7)) after it was corrected for changes in soil temperature and air pressure. Due to a small variation of soil moisture, soil CO_2 diffusion coefficient (Fig. 2e) did not vary significantly in the summer, although diurnal patterns were affected by soil temperature. Between days 200 and 235 D_s ranges from 2.29 to 2.54 $mm^2 s^{-1}$ with a mean of 2.43 $mm^2 s^{-1}$.

3.4. Soil CO_2 efflux and its correlation with soil temperature

After we measured soil CO_2 concentrations in the soil and estimated soil CO_2 diffusivity, we computed soil surface CO_2 efflux by Fick's law. Fig. 2b illustrates the seasonal variation of soil CO_2 efflux between days 200 and 235. Fig. 3b indicates the diurnal pattern of soil CO_2 efflux.

CO_2 efflux from the soil surface in the dry season at the savanna was very small. Between days 200 and 235, the daily mean values of CO_2 efflux slightly decreased from 0.43 to 0.33 $\mu mol\, m^{-2} s^{-1}$ with a mean of 0.37 $\mu mol\, m^{-2} s^{-1}$ or 0.0318 $mol\, m^{-2}$ per day. It corresponded with the small variation of daily mean soil temperature and moisture curves. Compared with the day-to-day variation (Fig. 2b), the mean diurnal range of CO_2 efflux (Fig. 3b) was greater within the study period, and correlated well with the diurnal variation of soil temperature (Fig. 3c).

The mean diurnal pattern of soil CO_2 efflux and its error bars (standard deviation) indicated a stable diurnal variation during this period. The diurnal variation of soil CO_2 efflux ranged from 0.32 ± 0.02 to $0.45 \pm 0.03\ \mu mol\, m^{-2} s^{-1}$. Soil CO_2 efflux increased after 09:00 h and reached the peak values at about 14:30–16:30 h. This pattern corresponded well with the increase in soil temperatures, particularly with the ones at depths of 8 and 16 cm. However, different from the diurnal temperature curves, which had one maximum value, the diurnal curve of soil CO_2 efflux had a small concave between 14:30 and 16:30 h. This may be caused by the decreased temperature sensitivity under very high temperature in the early afternoon. Microbial decomposition may be constrained by extremely high temperature and low moisture.

To investigate the temperature sensitivity (Q_{10} value) of soil CO_2 efflux at our site, we further plotted CO_2 efflux vs. soil temperature at the depth of 8 cm (Fig. 4). An exponential curve is fitted to the plot:

$$F = 0.162\, e^{0.0237T}, \qquad R^2 = 0.86, \quad n = 10\,090, \tag{9}$$

where F is the soil CO_2 efflux and T the soil temperature; $Q_{10} = 1.27$.

Eq. (9) indicates that CO_2 efflux has a strong correlation with soil temperature. The high correlation may be explained by the simple state of the system in which CO_2 efflux is derived mainly from heterotrophic respiration without the influence from root activities. During other times of the year soil CO_2 efflux will consist of root respiration and heterotrophic respiration. Its correlation with soil temperature may diminish then because root respiration (or total soil respiration) may also correlate with photosynthesis, as indicated by Kuzyakov and Cheng (2001) and Hogberg et al. (2001). Separately modeling heterotrophic respiration, tree root respiration, and grass root respiration in savannas are necessary because these three processes may be driven by different variables, parameters, and functional forms. It is suggested to further study root respiration from oak trees by comparing soil CO_2 efflux under trees (root and heterotrophic respirations combined) with one in the bare soil (heterotrophic respiration) in the summer.

Eq. (9) also indicates that the temperature sensitivity is relatively low in the dry season. The Q_{10} value is commonly considered ranging from 1.3 to 3.3 (Raich and Schlesinger, 1992). Q_{10} itself is also temperature-dependent (Lloyd and Taylor, 1994) and may positively correlate with moisture (Xu and Qi, 2001). The high temperature and extremely low moisture content in the summer at our site may explain the low Q_{10} value and low CO_2 efflux. This may be partially verified by the fact that the slightly decreased daily mean CO_2 efflux (Fig. 2b) responds to the slightly decreased daily mean moisture (Fig. 2d). The high correlation between CO_2 efflux and soil temperature may explain well the diurnal patterns of CO_2 efflux driven by soil temperature, but not seasonal patterns. It is expected that when moisture changes over seasons, moisture may become an important factor driving CO_2 efflux.

To study the seasonal pattern of soil CO_2 efflux and its sensitivity to soil temperature with varying soil

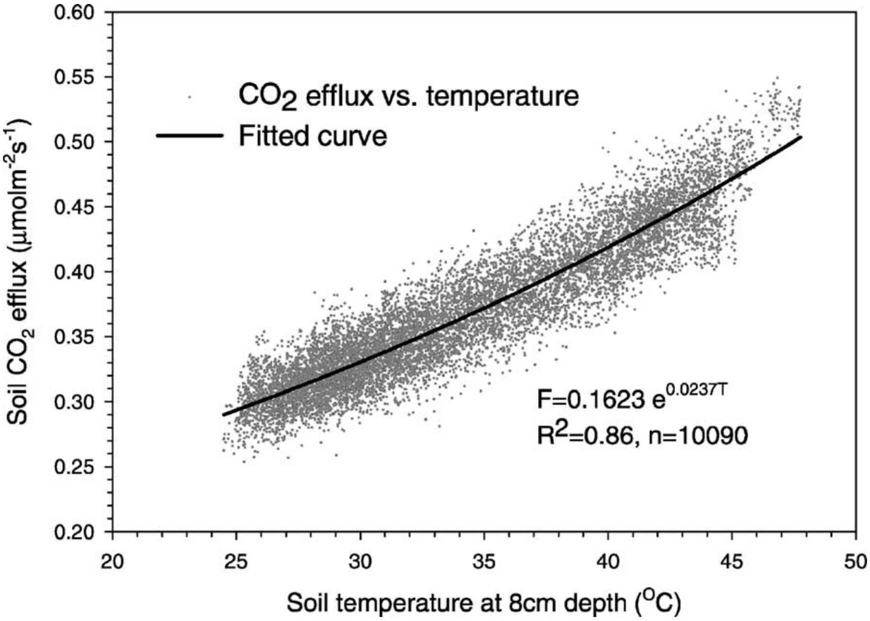

Fig. 4. Relationship between soil CO_2 efflux and temperature.

moisture contents, an extended measurement covering whole seasons is needed. The sensor probe and casing need to be protected from submerging in liquid water by some special coats which are still permeable for gaseous CO_2. The CO_2 gradient, which may not be a constant vertically, and diffusivity, which varies with moisture, can still be calculated using the methods we provided. Thus, by this approach continuous and long-term measurements of soil CO_2 efflux covering diurnal and seasonal variations become applicable.

By plotting soil CO_2 efflux with soil temperature at different depths, we found the correlation was the highest at the depth of 8 cm. The exponential curves of soil CO_2 efflux vs. soil temperature yielded R^2 of 0.78 and Q_{10} of 1.17 at the depth of 2 cm, and R^2 of 0.64 and Q_{10} of 1.54 at the depth of 16 cm. The highest correlation at 8 cm indicated that the soil temperature at this depth was suitable to study the relationship between CO_2 efflux and temperature. This may be the depth where most CO_2 was produced. The Q_{10} value increased with the depth of soil temperature measurements. Higher Q_{10} was found when temperature was measured at the deep soil than that measured at the top soil.

3.5. *Validation of CO_2 efflux*

To validate the estimated CO_2 efflux results, we used simultaneous and manually measured data to compare with estimated ones. A linear relationship was found between measured efflux and estimated one (using the Millington–Quirk diffusivity model) with a slope $= 0.907$, intercept $= -0.0348$, and $R^2 = 0.84$ (Fig. 5).

The estimated CO_2 efflux is correlated well with measured data, but it is about 9% less than the measured ones if the Millington–Quirk model is used. The way in which diffusivity was computed may explain this systematic difference. We selected the Millington–Quirk model to calculate the tortuosity factor ξ, or the ratio of gas diffusion coefficient (D_s/D_a). Sallam et al. (1984) plotted five models and compared the theoretical ratios including the Penman, Burger, Currie, Marshall, and Millington–Quirk models, in the order from the highest value of ξ to the lowest value. They found when the volumetric air content is less than 30%, the results of the Millington–Quirk model is the lowest compared with other models. To test the result from the Millington–Quirk model, we used the Marshall, the nearest model to the

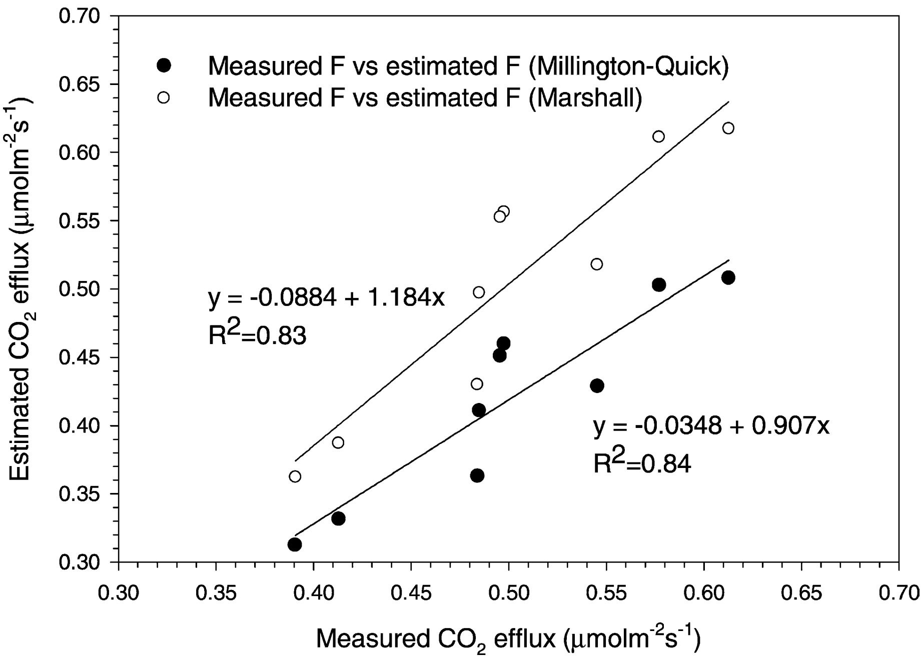

Fig. 5. Directly measured CO_2 efflux vs. estimated CO_2 efflux by gradient measurements and two diffusivity models, the Millington–Quirk and Marshall models. The two straight lines are fitted regression lines.

Millington–Quirk model, to compute diffusivity and then CO_2 efflux. As indicated in Fig. 5, the results from the Marshall model are systematically greater than measured ones by about 18%. The measured result falls between the Marshall and Millington–Quirk models. This may suggest that the difference between our estimated and measured effluxes comes from the diffusivity calculation, not from the CO_2 gradient measurement and computing. Further studies are suggested to modify the parameters of diffusivity models so that we may improve estimated CO_2 efflux results.

In addition to the validation of estimated CO_2 efflux, chamber measurements are able to complement the spatial variation of CO_2 efflux that is not captured by the miniature solid-state CO_2 sensors. The soil in the open area of the savanna is relatively homogeneous horizontally in the summer. Yet soil CO_2 efflux under oak trees is different from that in the open area. The spatial pattern will become more complex when grass is growing both under oak trees and in the open area in the rainy season. In order to understand both the spatial and temporal patterns of soil CO_2 efflux in the savanna, more deployments of CO_2 sensors in soils, horizontally and vertically, are suggested. Periodical chamber measurements also provide supplemental information on spatial variation.

Compared with chamber measurements which may disturb natural conditions such as air pressure, CO_2 gradient measurement methods do not cause this disturbance. Traditional gradient methods involve periodically extracting soil gas samples. The sensors and method introduced in this paper allow us to continuously measure CO_2 gradient without the need for gas extraction. This method is not influenced by wind velocity and flatness of terrains, which may cause biases for the eddy covariance technique. The potential errors for this gradient method may be from the unevenly distributed CO_2 sources in soils where the sensors are buried, and from the calculation of CO_2 diffusivity that varies temporally and spatially.

4. Conclusion

We described a simple technique to measure continuously soil CO_2 profile by burying small solid-state

CO_2 sensors at different soil depths. After calculating soil CO_2 diffusivity, we estimated CO_2 efflux, which was mainly from heterotrophic respiration, in a dry season in a Mediterranean savanna ecosystem in California. Between days 200 and 235 in 2002, the daily mean CO_2 concentration remained steady at 2 cm depth while slightly decreasing at 8 and 16 cm depth. The vertical CO_2 gradient at a certain time was approximately a constant when the depth was less than 16 cm, but the gradient varied over time. By running the Millington–Quirk model, we found soil CO_2 diffusion coefficient varied mainly with soil moisture. Ranging from 0.32 to 0.45 μmol m^{-2} s^{-1}, the diurnal pattern of CO_2 efflux was more significant than the day-to-day pattern.

CO_2 efflux had a strong exponential correlation with soil temperature at the depth of 8 cm with R^2 of 0.86 and Q_{10} of 1.27 in the summer dry season. The Q_{10} value increased with soil depth of temperature measurements. The extremely low moisture content in the summer at our site may explain the low Q_{10} value. The high correlation between soil CO_2 efflux and temperature may be due to the minimum disturbance and continuous measurements of heterotrophic respiration from soils. The high correlation explains the diurnal patterns of CO_2 efflux driven by soil temperature, but it is expected that moisture may become an important factor driving CO_2 efflux when moisture changes over seasons.

By comparing estimated CO_2 efflux with measured CO_2 efflux data, we conclude that the described CO_2 sensors and diffusion method yielded satisfactory results. This simple and commercially available technique provides continuous soil CO_2 concentration profiles, and thus helps us estimate CO_2 production at various depths of soils and efflux from the soil surface. It may also help to decompose NEP and calibrate and correct eddy covariance data.

Acknowledgements

We thank Ted Hehn and Dick Gronholm for the technical help in setting instruments, and Nicole Baldocchi for helping draw Fig. 1. We thank two anonymous reviewers and Riccardo Valentini for constructive comments on the manuscript. We also thank Mr. Russell Tonzi for access and use of his ranch. JT is partly supported by Edward A. Colman Fellowship and W.S. Rosecrans Fellowship at UC Berkeley. DDB acknowledges support by DOE/TCP and the California Agricultural Experiment Station.

References

Baldocchi, D.D., Meyers, T.P., 1991. Trace gas-exchange above the floor of a deciduous forest. 1. Evaporation and CO_2 efflux. J. Geophys. Res.: Atmos. 96, 7271–7285.

Baldocchi, D., et al., 2001. FLUXNET: a new tool to study the temporal and spatial variability of ecosystem-scale carbon dioxide, water vapor, and energy flux densities. Bull. Am. Meteorol. Soc. 82, 2415–2434.

Burton, D.L., Beauchamp, E.G., 1994. Profile nitrous-oxide and carbon-dioxide concentrations in a soil subject to freezing. Soil Sci. Soc. Am. J. 58, 115–122.

Cox, P.M., Betts, R.A., Jones, C.D., Spall, S.A., Totterdell, I.J., 2000. Acceleration of global warming due to carbon-cycle feedbacks in a coupled climate model. Nature 408, 750–750.

Davidson, E.A., Trumbore, S.E., 1995. Gas diffusivity and production of CO_2 in deep soils of the eastern Amazon. Tellus Ser. B: Chem. Phys. Meteorol. 47, 550–565.

Davidson, E.A., Belk, E., Boone, R.D., 1998. Soil water content and temperature as independent or confounded factors controlling soil respiration in a temperate mixed hardwood forest. Global Change Biol. 4, 217–227.

Davidson, E.A., Savage, K., Verchot, L.V., Navarro, R., 2002. Minimizing artifacts and biases in chamber-based measurements of soil respiration. Agric. For. Meteorol. 113, 21–37.

De Jong, E., Schapper, H.J.V., 1972. Calculation of soil respiration and activity from CO_2 profiles in soil. Soil Sci. 113, 328–333.

Drewitt, G.B., et al., 2002. Measuring forest floor CO_2 fluxes in a Douglas-fir forest. Agric. For. Meteorol. 110, 299–317.

Epron, D., Farque, L., Lucot, E., Badot, P.M., 1999. Soil CO_2 efflux in a beech forest: dependence on soil temperature and soil water content. Ann. For. Sci. 56, 221–226.

Giardina, C.P., Ryan, M.G., 2000. Evidence that decomposition rates of organic carbon in mineral soil do not vary with temperature. Nature 404, 858–861.

Goulden, M.L., Crill, P.M., 1997. Automated measurements of CO_2 exchange at the moss surface of a black spruce forest. Tree Physiol. 17, 537–542.

Goulden, M.L., Munger, J.W., Fan, S.M., Daube, B.C., Wofsy, S.C., 1996. Measurements of carbon sequestration by long-term eddy covariance: methods and a critical evaluation of accuracy. Global Change Biol. 2, 169–182.

Hanson, P.J., Edwards, N.T., Garten, C.T., Andrews, J.A., 2000. Separating root and soil microbial contributions to soil respiration: a review of methods and observations. Biogeochemistry 48, 115–146.

Healy, R.W., Striegl, R.G., Russell, T.F., Hutchinson, G.L., Livingston, G.P., 1996. Numerical evaluation of static-chamber measurements of soil–atmosphere gas exchange: identification of physical processes. Soil Sci. Soc. Am. J. 60, 740–747.

Hirano, T., Setoyama, H., Tanaka, Y., Kim, H., 2000. Diffusive CO_2 efflux from the soil surface of a deciduous broad-leaved forest in Hokkaido, Japan. In: Proceedings of the International Workshop for Advanced Flux Network and Flux Evaluation. Center for Global Environmental Research, National Institute for Environmental Studies, Japan, pp. 113–118.

Hogberg, P., et al., 2001. Large-scale forest girdling shows that current photosynthesis drives soil respiration. Nature 411, 789–792.

Jones, H.G., 1992. Plants and Microclimate: A Quantitative Approach to Environmental Plant Physiology. Cambridge University Press, New York, p. 51.

Jury, W.A., Gardner, W.R., Gardner, W.H., 1991. Soil Physics. Wiley, New York, pp. 209–210.

Kiang, N., 2002. Stomatal control under drought: a function of landscape optimization. Ph.D. Dissertation. University of California, Berkeley.

King, J.A., Harrison, R., 2002. Measuring soil respiration in the field: an automated closed chamber system compared with portable IRGA and alkali absorption methods. Commun. Soil Sci. Plant Anal. 33, 403–423.

Kirschbaum, M.U.F., 1995. The temperature dependence of soil organic matter decomposition, and the effect of global warming on soil organic C storage. Soil Biol. Biochem. 27, 753–760.

Kirschbaum, M.U.F., 2000. Will changes in soil organic carbon act as a positive or negative feedback on global warming? Biogeochemistry 48, 21–51.

Kuzyakov, Y., Cheng, W., 2001. Photosynthesis controls of rhizosphere respiration and organic matter decomposition. Soil Biol. Biochem. 33, 1915–1925.

Law, B.E., Baldocchi, D.D., Anthoni, P.M., 1999. Below-canopy and soil CO_2 fluxes in a ponderosa pine forest. Agric. For. Meteorol. 94, 171–188.

Law, B.E., et al., 2001. Spatial and temporal variation in respiration in a young ponderosa pine forests during a summer drought. Agric. For. Meteorol. 110, 27–43.

Liski, J., Ilvesniemi, H., Makela, A., Westman, C.J., 1999. CO_2 emissions from soil in response to climatic warming are overestimated—the decomposition of old soil organic matter is tolerant of temperature. Ambio 28, 171–174.

Livingston, G.P., Hutchinson, G.L., 1995. Enclosure-based measurement of trace gas exchange: applications and sources of error. In: Harriss, R.C. (Ed.), Biogenic Trace Gases: Measuring Emissions from Soil and Water. Blackwell Scientific Publications, London, pp. 14–51.

Lloyd, J., Taylor, J.A., 1994. On the temperature-dependence of soil respiration. Funct. Ecol. 8, 315–323.

Luo, Y.Q., Wan, S.Q., Hui, D.F., Wallace, L.L., 2001. Acclimatization of soil respiration to warming in a tall grass prairie. Nature 413, 622–625.

Massman, W.J., et al., 1997. A model investigation of turbulence-driven pressure-pumping effects on the rate of diffusion of CO_2, N_2O, and CH_4 through layered snowpacks. J. Geophys. Res.: Atmos. 102, 18851–18863.

Meyer, W.S., Reicosky, D.C., Barrs, H.D., Shell, G.S.G., 1987. A portable chamber for measuring canopy gas exchange of crops subject to different root zone conditions. Agron. J. 79, 181–184.

Millington, R., Quirk, J.P., 1961. Permeability of porous solids. Trans. Faraday Soc. 57, 1200–1207.

Moncrieff, J., Valentini, R., Greco, S., Seufert, G., Ciccioli, P., 1997. Trace gas exchange over terrestrial ecosystems: methods and perspectives in micrometeorology. J. Exp. Bot. 48, 1133–1142.

Norman, J.M., Garcia, R., Verma, S.B., 1992. Soil surface CO_2 fluxes and the carbon budget of a grassland. J. Geophys. Res.: Atmos. 97, 18845–18853.

Piovesan, G., Adams, J.M., 2000. Carbon balance gradient in European forests: interpreting EUROFLUX. J. Veg. Sci. 11, 923–926.

Raich, J.W., Schlesinger, W.H., 1992. The global carbon-dioxide flux in soil respiration and its relationship to vegetation and climate. Tellus Ser. B: Chem. Phys. Meteorol. 44, 81–99.

Russell, C.A., Voroney, R.P., Black, T.A., Blanken, P.D., Yang, P.C., 1998. Carbon dioxide efflux from the floor of a boreal aspen forest. II. Evaluation of methods—verification by infra-red analysis of a dynamic closed chamber. Can. J. Soil Sci. 78, 311–316.

Sallam, A., Jury, W.A., Letey, J., 1984. Measurement of gas-diffusion coefficient under relatively low air-filled porosity. Soil Sci. Soc. Am. J. 48, 3–6.

Scott, A., Crichton, I., Ball, B.C., 1999. Long-term monitoring of soil gas fluxes with closed chambers using automated and manual systems. J. Environ. Qual. 28, 1637–1643.

Singh, J.S., Gupta, S.R., 1977. Plant decomposition and soil respiration in terrestrial ecosystems. Bot. Rev. 43, 449–528.

Treonis, A.M., Wall, D.H., Virginia, R.A., 2002. Field and microcosm studies of decomposition and soil biota in a cold desert soil. Ecosystems 5, 159–170.

Trumbore, S.E., Chadwick, O.A., Amundson, R., 1996. Rapid exchange between soil carbon and atmospheric carbon dioxide driven by temperature change. Science 272, 393–396.

Wagner, G.H., Buyanovsky, G.A., 1983. Use of gas sampling tubes for direct measurement of CO_2-C14 in soil air. Int. J. Appl. Radiat. Isotopes 34, 645–648.

Xu, M., Qi, Y., 2001. Spatial and seasonal variations of Q_{10} determined by soil respiration measurements at a Sierra Nevadan forest. Global Biogeochem. Cycles 15, 687–696.